

A Poor's Man Approach to Solar Radio Emission Characterization

F. Sapienza⁽¹⁾, F. Giannetti*⁽¹⁾, and A. Vaccaro⁽²⁾

(1) Department of Information Engineering, University of Pisa, 56122, Pisa, Italy (filippo.giannetti@unipi.it)

(2) M.B.I. S.r.l., 56121, Pisa, Italy

Abstract

The Sun (both the photosphere and the corona) is a strong source of radiation across the entire RF spectrum. Under some particular circumstances, Sun noise may heavily interfere with ground receivers for communication satellites or deep space probes, causing degradation, or even destruction, of the useful signal. An accurate characterization of the solar noise is therefore of great importance, especially in the design of satellite broadcasting systems or deep space missions. In this paper we experimentally investigate the transit of the Sun behind a broadcasting satellite by resorting to a commercial-grade receiving equipment for satellite TV and we numerically assess the amount of radiated noise. Experimental results are eventually validated by a comparison with data collected by NASA's deep-space missions.

1. Introduction

The Sun is a strong source of radiation across the entire radio frequency (RF) spectrum, originating from both the photosphere and the corona. In some particular circumstances, the Sun may heavily interfere with the (weak) microwave (μW) signal received by an Earth station (ES) and arriving from either a communication satellite on a geocentric orbit, or a deep-space probe travelling across the Solar System. For instance, the downlink of a communication geostationary satellite (GEOS) for direct-to-home (DTH) TV broadcasting (or broadband access), in C, or Ku, or Ka bands, experiences interference when the Sun, during its apparent motion across the sky, enters the beam of the ES antenna (a satellite TV dish), and from ground it is seen to pass behind the satellite [1]; this phenomenon is usually termed "Sun transit" (Figure 1). In the case of a deep-space mission, instead, the ES, typically one of NASA's Deep Space Network (DSN) stations equipped with a large-size, high-gain, and narrow-beam antenna, may occasionally see the probe (e.g., the Voyager 1/2) nearly in conjunction with the Sun, i.e., at low Sun Earth probe (SEP) angles. Then, the ES antenna, aimed at the probe, will catch additional RF noise from the solar corona, affecting the reception of the probe's signal in the X, or Ka bands. In both the cases, the Sun causes a noise increase in the ground receiver, termed Sun noise temperature (SNT) T_S (in Kelvin), which sums up to the

background noise, i.e., cosmic, atmospheric, ground and receiver electronics contributions. The detrimental effects of SNT can be partial degradation, i.e., signal-to-noise ratio (SNR) reduction and error rate increase, or even outage (i.e., total destruction of the useful signal), and this is why this phenomenon is also known as "Sun fade" or "Sun outage". An accurate characterization of the SNT is of great importance in the following applications. i) GEOS-based broadcasting – The SNT can be used in the design of the downlink [2], for Sun fade/outage prediction. ii) Opportunistic rainfall estimate – The attenuation measurement in GEOS downlinks can be used to derive a real-time estimate of rainfall intensity (in mm/h) along the signal path [3]. This feature reveals especially appealing for now-casting services and climate change monitoring (e.g., the H2020 SCORE project, <https://score-eu-project.eu>) and, as such, it requires accurate real-time measurements of the received SNR and prompt management of spurious, i.e., non-rain related, alterations of SNR which may cause false detection of rain events. iii) Deep-space missions – The SNT is necessary for the evaluation of the lowest SEP angle allowing a reliable link from the probe to the ES through the solar corona, and the duration of the communication blackout during the transit of the probe behind, or in front of, the Sun.

In this paper we experimentally investigate the transit of the Sun behind a broadcasting GEOS, and we numerically assess the SNT in Ku-band, by resorting to a simple commercial-grade DTH receiving equipment. Experimental results are eventually validated by a comparison with data collected by NASA's deep-space missions.

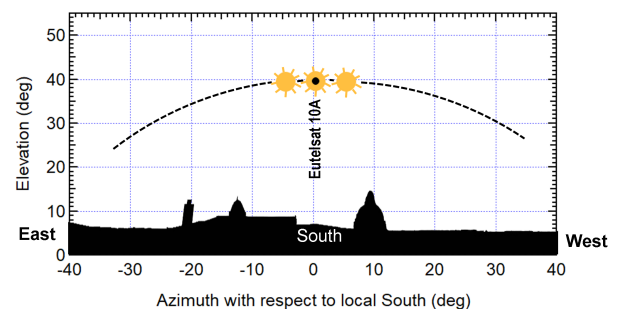


Figure 1. Sun transit, at 15 minute-steps, behind GEOS Eutelsat 10A, 10°E, in Pisa, Italy. Sun diameter is not to scale. The Dashed line is the arc of the GEOSs.

2. Measurement System

The measurements presented in this work have been made by two ESs located in Northern Tuscany, Italy, (Figure 2, right), which are part of a sensor network deployed across Central Italy during the Nefocast project [4]. The standard time of both the ES locations is UTC+1; their ID and coordinates are listed in Table 1. The measurement equipment in each ESs consists of a commercial-grade receiver for DTH digital video broadcasting - satellite 2nd gen. (DVB-S2) and a conventional parabolic dish. Both the Nefocast ESs were aimed at the Eutelsat 10A satellite, in 10°E orbital position (Figure 1).

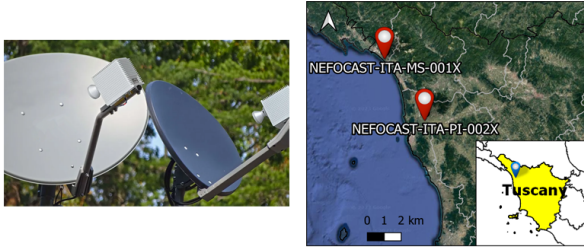


Figure 2. IoT FIRST terminals and offset satellite dishes (left). Location of the 2 Nefocast ESs in Tuscany (right).

Table 1. ID and coordinates of the Nefocast ESs.

ES ID	Lon (°N)	Lat (°E)	City
NEFOCAST-ITA-MS-001X	44.0344	10.1402	Massa
NEFOCAST-ITA-PI-002X	43.6962	10.4277	Pisa

2.1. IoT FIRST Terminal and Platform

The satellite terminal, called IoT FIRST and produced by AYECKA Ltd., Israel (www.ayecka.com), is an innovative low-cost and small-size device, which integrates into the same compact case both the low-noise block converter (LNB) and the decoder functionalities. Thanks to its optimized form-factor, the IoT FIRST device can be mounted in the focus of a conventional offset dish (Figure 2 left). The IoT FIRST is a two-way (i.e., transmit/receive) device that enables the following links, providing support for both interactive TV services and Internet of things (IoT) / machine-to-machine (M2M) applications:

- i) forward link (FL) reception – satellite to ground down-link in the 10-13 GHz Ku-band, featuring DVB-S2 receiver;
- ii) return link (RL) transmission – ground to satellite up-link in the 14 GHz Ku-band carrying the receiver status, including the FL SNR plus IoT sensor data, featuring a low-power ground-to-satellite transmitter.

The SNR measurements presented in this work have been made on the FL signal, whose parameters are listed in Table 2. The RL enables the receiver to send these SNR measurements to a remote data collection and fusion center, via the EURO BIS IoT First platform and using the same Eutelsat 10A satellite (Figure 1). [4].

Table 2. Main parameters of the FL from Eutelsat 10A.

Parameters	Value
EIRP	48 dBW
FL frequency	11.345 GHz
FL polarization	vertical
modcod format	QPSK 4/5

2.2. Receiving Antenna

The Nefocast ES receiving antenna is a conventional off-set dish with diameter 80 cm for satellite DTH TV reception. Assuming an efficiency 0.7, the gain along the boresight is $G_R = 38$ dBi and the -3 dB beamwidth is $\theta_{3dB} = 2.32^\circ$, as shown in Figure 3 (see [2], Sect. 5.2, eqns. (5.3)–(5.4b)).

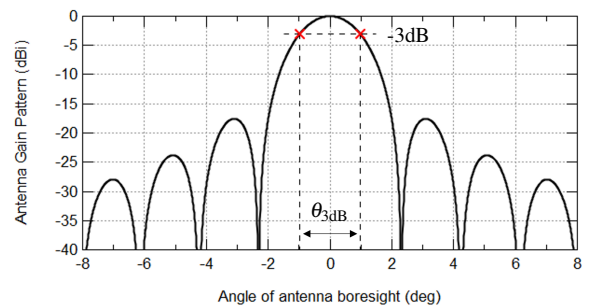


Figure 3. Gain pattern of a 80 cm dish.

3. Sun Transit

Twice a year, around equinoxes [1], Sun transits cause deep notches on the SNR measured at the satellite receiver. For a 80 cm-diameter dish, every notch has a duration of about 20 minutes and occurs every day over a period of a dozen of days. In the Northern Hemisphere this phenomenon happens a few days before the March equinox and a few days after the September equinox, while in the Southern Hemisphere it happens after the March equinox and before the September equinox. The actual number of days in advance or delay w.r.t. the equinoxes depends on the ES latitude (see Figure 4).

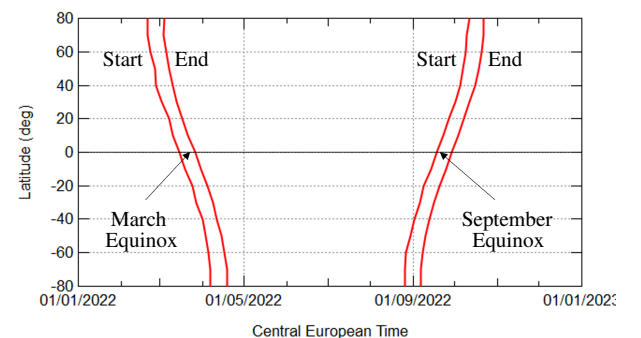


Figure 4. Start/end dates of Sun transit periods.

4. Datasets

We used the following three different datasets containing SNR readings from the satellite Eutelsat 10A at 10°E, taken every minute during the March and September equinoxes by the IoT FIRST receivers of the two Nefocast ESs:

- dataset A: collected by NEFOCAST-ITA-MS-001X from Feb. 26 to Mar. 7, 2022;
- dataset B: collected by NEFOCAST-ITA-PI-002X from Feb. 26 to Mar. 7, 2022;
- dataset C: collected by NEFOCAST-ITA-MS-001X from Oct. 6 to Oct. 15, 2022.

The SNR readings are in the form of the ratio $\eta = E_s/N_0$, wherein E_s is the average RF received energy during one QPSK symbol interval and N_0 is the one-sided noise power spectral density (PSD) [4]. For the sake of exemplification, the SNR measurements in dataset A, plotted in Figure 5 exhibit a series of deep notches caused by Sun transits, occurring daily around 11:30 UTC (12:30 local time). Actually, the Nefocast ES and the satellite have almost the same longitude, so the transits occur around local noon.

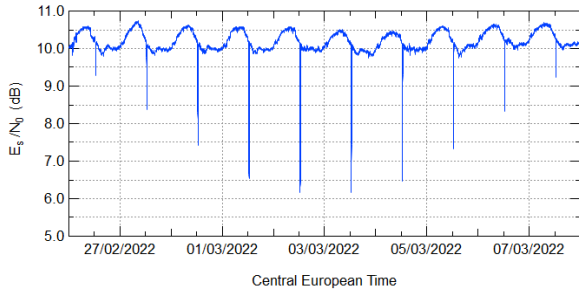


Figure 5. Time plot of dataset A.

5. Solar Noise Temperature Derivation

Let denote with:

- $t_n = n\tau$ the n th sampling instant of the receiver, where τ is the sampling interval (1 minute);
- $t_{start} = i_0\tau$ and $t_{stop} = i_1\tau$, with i_0 and i_1 integers, the start and the end instants of the notch, respectively;
- $E_s(n\tau)$ the received energy per symbol (it is time-varying, due to residual orbit inclination);
- $T_{MGR} = T_M \left(\frac{L-1}{L}\right) + T_G + T_R$ the total noise temperature without extra-terrestrials sources, where T_M , T_G , and T_R are the noise temperatures of meteorological formations, ground and receiver hardware, respectively, and L is the atmospheric attenuation;
- N_0 the one-sided PSD of the noise [4] without the contribution of the Sun, expressed as

$$N_0 = k_B \left(\frac{T_C}{L} + T_{MGR} \right), \quad (1)$$

where k_B is the Boltzmann constant and T_C is the noise temperature of the cosmic background;

- $N_0^{(S)}(n\tau)$ the time-varying one-sided PSD of the noise, including the Sun noise from both photosphere and corona, or from corona only, expressed as

$$N_0^{(S)}(n\tau) = k_B \left[\frac{T_C + T_S(n\tau)}{L} + T_{MGR} \right]; \quad (2)$$

- $\eta^{(S)}(n\tau) = E_s(n\tau)/N_0^{(S)}(n\tau)$ the samples of the SNR during the Sun transit;
- $\eta^{(ref)}(n\tau)$ the reference SNR level, which is calculated by linear interpolation between the sample at the start of the transit $\eta(t_{start})$ and the one at the end $\eta(t_{stop})$ (red marks in Figure 6), and can be expressed as $\eta^{(ref)}(n\tau) = E_s(n\tau)/N_0$.

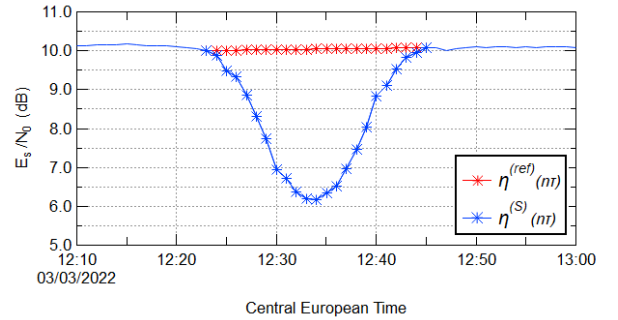


Figure 6. Record of SNR from Eutelsat 10A during a Sun transit (blue marks) and reference SNR level for the evaluation of the excess noise (red marks).

Table 3. Parameters of the noise PSD.

Parameters	Value
L	0.09 dB
T_C	2.78 K
T_M	275 K
T_G	45 K
T_R	13.67 K

The numerical values of the parameters that appear in PSD expressions (1) and (2) are reported in Table 3. From vii) and viii), with some manipulations, we obtain the SNT picked-up by the receiving antenna during the transit

$$T_S(n\tau) = N_0 \frac{L}{k_B} \left[\frac{\eta^{(ref)}(n\tau)}{\eta^{(S)}(n\tau)} - 1 \right]. \quad (3)$$

According to (3), Figure 7 shows the peak values of the SNT for the ten transits observed in Massa, near the March 2022 equinox (dataset A), while Table 4 reports the peak values of all the three datasets. Notice that, by plotting the apparent trajectory of the Sun in the sky, and taking into account both the apparent diameter of the Sun and the antenna beamwidth, it can be verified that the first and the last peaks of each dataset, reported in bold in the Table, are due to the effect of the solar corona only, as the photosphere appears to transit outside the antenna spot (not shown here due to lack of space).

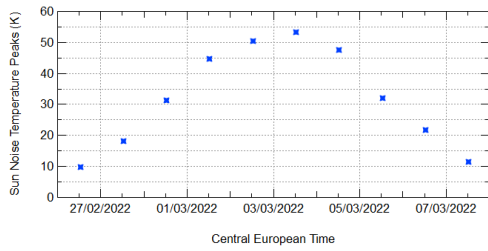


Figure 7. Peaks of SNT from dataset A.

Table 4. Peaks of SNT for the three datasets (in bold, noise peaks due to solar corona only).

Date	T_S peak (K), City-Datset	
Feb. 26, 2022	9.69 , Massa-A	9.38 , Pisa-B
Feb. 27, 2022	18.24, Massa-A	16.76, Pisa-B
Feb. 28, 2022	31.23, Massa-A	25.23, Pisa-B
Mar. 1, 2022	44.77, Massa-A	32.27, Pisa-B
Mar. 2, 2022	50.42, Massa-A	36.28, Pisa-B
Mar. 3, 2022	53.27, Massa-A	38.25, Pisa-B
Mar. 4, 2022	47.56, Massa-A	33.24, Pisa-B
Mar. 5, 2022	31.94, Massa-A	23.46, Pisa-B
Mar. 6, 2022	21.83, Massa-A	16.78, Pisa-B
Mar. 7, 2022	11.48 , Massa-A	8.74 , Pisa-B
Oct. 6, 2022	7.25 , Massa-C	
Oct. 7, 2022	16.09, Massa-C	
Oct. 8, 2022	27.06, Massa-C	
Oct. 9, 2022	36.09, Massa-C	
Oct. 10, 2022	40.08, Massa-C	
Oct. 11, 2022	43.08, Massa-C	
Oct. 12, 2022	37.08, Massa-C	
Oct. 13, 2022	25.61, Massa-C	
Oct. 14, 2022	16.42, Massa-C	
Oct. 15, 2022	7.08 , Massa-C	

6. Comparison with space missions data

Table 5 reports the SNT measured in Ku-band by the two Nefocast ESs (on Mar. 3 and Oct. 11, 2022) and the measurements made by NASA's DSN station DSS-43 with a 64 m-diameter highly-directive antenna, at a frequency of 8240 MHz (X-band), during a solar conjunction of the Voyager 1 and 2 probes in late Dec. 1987 [5]. For both the cases, data are reported for SEP angles greater than 1.59° . This implies that the pencil-beam of DSS-43 antenna picked up noise only from small spots in the corona (i.e., outside the apparent diameter of the Sun). Similarly, the 2.32° -wide beam of the satellite TV dish used by the Nefocast ESs was entirely in the corona, too. The higher SNT values measured by the Nefocast ESs could be due to the much larger beamwidth that caught a certain amount of radiation also from the inner, and noisier too, part of the solar corona (i.e., that closer to the photosphere).

7. Conclusions

The numerical assessment of the radiated solar noise is important in satellite broadcasting design, opportunistic rain estimation and deep space missions. We measured the Ku-band SNT during the transits around the equinoxes in 2022, using only a small dish for satellite TV, and the results were compared with those collected by Voyager missions. Further work is needed to assess the sensitivity of the results w.r.t. solar activity and the 11-year sunspot cycle. The low-cost receiving setup employed here also renders this approach suited for educational activities and research projects with citizen science campaigns.

Table 5. Comparison of the measured SNT on Mar. 3 and Oct. 11, 2022, with Voyager data obtained at DSS-43 during solar conjunction of Dec. 1987.

Receiving ES	Time	SEP Angle	T_S (K)	Band
Massa	Oct. 11, 2022	1.59°	19.73	Ku
DSS-43	Dec. 1987	1.60°	6	X
Massa	Mar. 3, 2022	1.60°	20.87	Ku
Pisa	Mar. 3, 2022	1.61°	21.37	Ku
DSS-43	Dec. 1987	1.63°	3	X
DSS-43	Dec. 1987	1.73°	22	X

Acknowledgements

This paper is based upon work from COST Action OpenSense CA20136 and was supported by the following projects: SCORE (Smart Control of the Climate Resilience in European Coastal Cities), funded by the European Commission's Horizon 2020 programme under grant agreement No. 101003534; FoReLab (Departments of Excellence), funded by the Italian Ministry of Education and Research (MUR). The fruitful cooperation with the partners of the INSIDERAIN project is acknowledged.

References

- [1] J. Vankka and A. Kestilä, "Sun outage calculator for geostationary orbit satellites," *Jurnal Kejuruteraan*, no. 26, pp. 21–30, 2014.
- [2] G. Maral, M. Bousquet, and Z. Sun, *Satellite Communications Systems, 5th ed.* John Wiley & Sons Inc., 2010.
- [3] F. Giannetti and R. Reggiannini, "Opportunistic rain rate estimation from measurements of satellite downlink attenuation: A survey," *Sensors*, 2021, vol. 21, no. 17,
- [4] F. Giannetti et alii, "The nefocast system for detection and estimation of rainfall fields by the opportunistic use of broadcast satellite signals," *IEEE AES Mag.*, vol. 34, no. 6, pp. 16–27, 2019.
- [5] T. A. Rebold and T. K. Peng, "X-band noise temperature near the sun at a 34-meter high efficiency antenna." (1988), [Online]. Available: https://ipnpr.jpl.nasa.gov/progress_report/42-93/93V.PDF.